Earth and Planetary Science Letters 405 (2014) 110–118

Contents lists available at ScienceDirect

Earth and Planetary Science Letters

www.elsevier.com/locate/epsl

Driving the upper plate surface deformation by slab rollback and mantle flow

Pietro Sternai [a,*], Laurent Jolivet [a], Armel Menant [a], Taras Gerya [b]

[a] Institut de Sciences de la Terre d'Orléans (ISTO), University of Orléans, France
[b] Institute of Geophysics, Swiss Federal Institute of Technology (ETH), Zürich, Switzerland

ARTICLE INFO

Article history:
Received 19 March 2014
Received in revised form 22 July 2014
Accepted 17 August 2014
Available online 14 September 2014
Editor: Y. Ricard

Keywords:
slab tearing
slab rollback
mantle flow
surface deformation

ABSTRACT

The relative contribution of crustal and mantle processes to surface deformation at convergent plate margins is still controversial. Conflicting models involving either extrusion mechanisms or slab rollback, in particular, were proposed to explain the surface strain and kinematics across the Tethyan convergent domain. Here, we present new high-resolution 3D thermo-mechanical numerical joint models of continental collision, oceanic subduction and slab tearing, which for the first time allow self-consistent reproduction of first-order Tethyan tectonic structures such as back-arc rifting and large-scale strike-slip faults accommodating continental escape. These models suggest that mantle flow due to slab rollback and tearing can modulate the surface strain and kinematics by locally enhancing trench retreat and dragging the upper plate from below. These results highlight the active role of the asthenospheric flow in driving the surface strain, not only by modulating the vertical stresses and producing dynamic topography but also through sub-horizontal motion. We discuss the implications of these findings based on observations across the Aegean–Anatolian and eastern Indian–Eurasian domains, though similar considerations may as well apply to other settings.

1. Introduction

Plate fragmentation, mountain building, formation of extensional basins, and major strike-slip fault zones characterised the long-term evolution of the Tethyan convergent domains (e.g., Ricou, 1994). Surface deformation is classically attributed to either collision-related processes such as crustal shortening, extrusion and gravitational spreading (e.g., Tapponnier and Molnar, 1976; Le Pichon et al., 1992) or subduction-related mechanisms such as slab pull or rollback and trench retreat (e.g., Dewey, 1988; Royden, 1993). However, subduction of the Tethyan lithosphere and collision along the African, Arabian, Indian and Eurasian margins often coexisted, interacting with each other to set jointly the surface kinematics and strain.

For instance, oceanic subduction below the Hellenic domain coexisted with active convergence across the neighbouring Bitlis–Zagros region since approximately the late Oligocene (e.g., Sengör, 1979; Jolivet and Faccenna, 2000; Allen et al., 2004). GPS measurements show a westward motion of Anatolia and a southward propagation of the Hellenic trench with respect to Eurasia (Reilinger et al., 2010), resulting in an overall counter-clockwise rotation (Fig. 1a). Most of this rotation is accommodated by the north-Anatolian fault (NAF), a strike-slip fault zone joining the Bitlis–Zagros domain to the east and the Aegean/Hellenic extensional back-arc region to the west (e.g., McKenzie, 1972; Sengör, 1979; Armijo et al., 1999). Tomographic models (Li et al., 2008a) show a low-velocity anomaly below western Turkey, which was interpreted as a major tear in the Hellenic slab (De Boorder et al., 1998; Govers and Wortel, 2005) (Fig. 1b). Recent studies foster the hypothesis that the mantle flow induced by slab rollback codetermines the surface deformation (Faccenna et al., 2006, 2013a, 2013b; Jolivet et al., 2009, 2013; Pérouse et al., 2012).

Another example spanning larger scales and a longer temporal evolution is south-eastern Asia in which collision of India with Eurasia and the Andaman–Sumatra subduction contribute jointly to surface deformation across the Himalaya, Indochina and Indonesia since ~45 Ma (e.g., Royden, 1997; Tapponnier et al., 2001; Royden et al., 2008; Replumaz et al., 2013). Geodetic measurements relative to stable Eurasia show a prominent clockwise rotation around the Eastern Himalayan Syntaxes (EHS) characterised by eastward motion of eastern Tibet and western Sichuan, south-eastward motion in northern Yunan and south to south-eastward motion in southern Yunan (Zhang et al., 2004; Gan et al., 2007; ArRajehi et al., 2010) (Fig. 1c). Several strike-slip fault zones, which arrange from the convergent domain north of Tibet, such as the

* Corresponding author.
E-mail address: pietro.sternai@univ-orleans.fr (P. Sternai).

http://dx.doi.org/10.1016/j.epsl.2014.08.023
0012-821X/

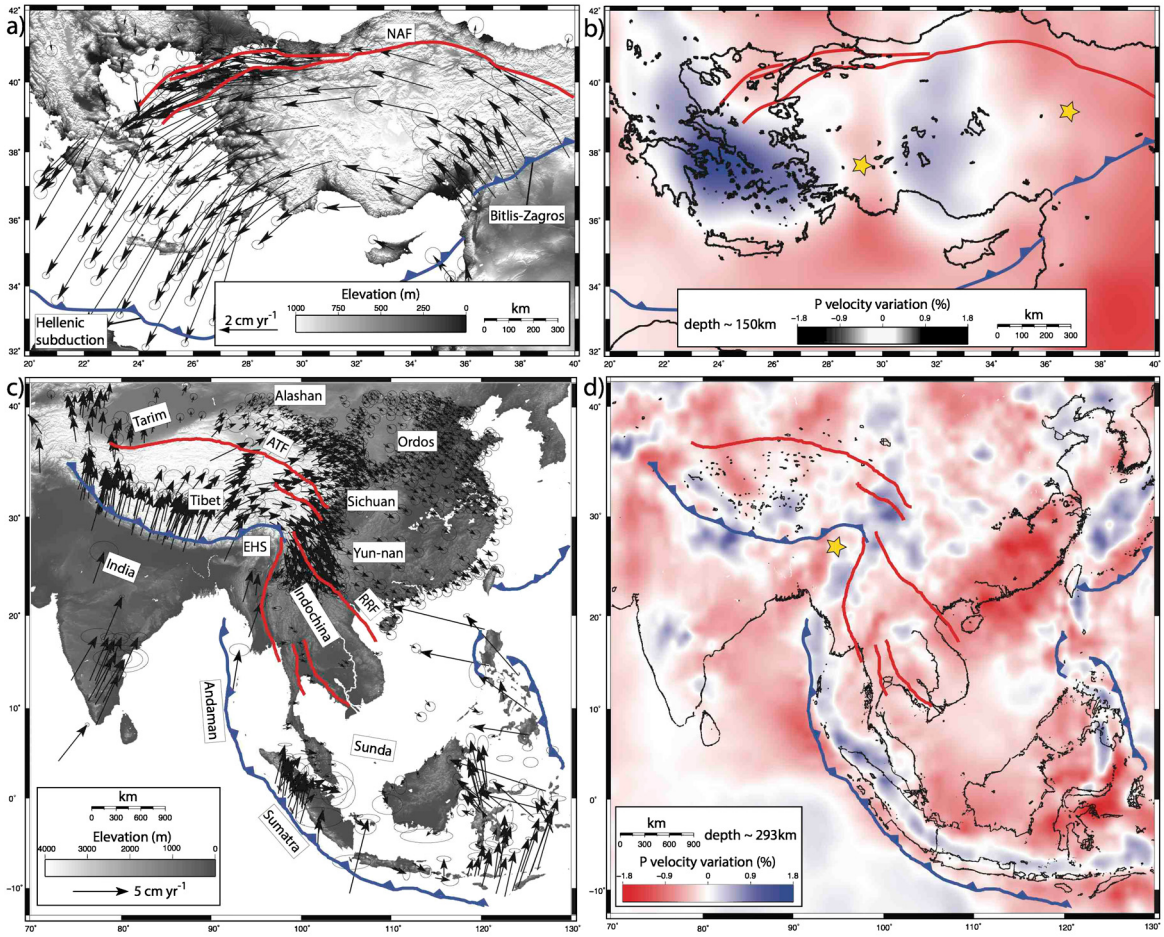

Fig. 1. Maps of the Aegean–Anatolian and Indian–Eurasian systems. a, c) Topography and GPS velocities with 95% confidence ellipses (Zhang et al., 2004; Gan et al., 2007; Reilinger et al., 2010). b, d) Tomographic models (Li et al., 2008a) showing the V_p anomalies at the depths indicated. Stars show the locations of slab tears. Red and blue lines in all panels represent the major strike-slip fault zones and thrusts and subduction fronts, respectively.

Altyn-Tagh Fault, to the extensional domain east and south of it, such as the Red River Fault (RRF), accommodate the majority of this motion (e.g., Molnar and Tapponnier, 1975; Tapponnier and Molnar, 1976). Several basins, such as the South China Sea, have developed east of Tibet and offshore the Indochina peninsula in the Oligocene and Miocene (Tapponnier et al., 1982, 1986; Taylor and Hayes, 1983). The main direction of extension across these regions was N–S and the relationships between the formation of these basins and large-scale shear zones such as the RRF have been widely debated: these topographic lows formed either as a pull-apart basin at the south-easternmost extremity of the RRF (i.e., extrusion: e.g., Tapponnier et al., 1982, 1986) or as more classical back-arc basins behind the retreating subduction (i.e., slab retreat: e.g., Taylor and Hayes, 1983; Jolivet et al., 1994; Fournier et al., 2004). The deep mantle structures associated with subduction of ancient Tethyan lithosphere vary significantly along the collision boundary (Fig. 1d). In particular, while deep and shallow slabs may be still (spatially) connected in the central Himalayas (Li et al., 2008a, 2008b), there is no evidence for such a connection beneath the eastern Himalayas. Tomographic images show a low velocity zone below the EHS at depth larger than ~200 km separating the Indian and Andaman–Sumatra slabs (Li et al., 2008a). This slab tear might have facilitated southward to westward rollback of the Andaman–Sumatra subduction after the onset of collision between India and Eurasia, and the mantle flow through the slab window and around the EHS might have codetermined the surface strain (Fig. 1c, d) (Holt, 2000).

Conflicting models involving extrusion tectonics originated by the Arabia/India–Eurasia collision or rollback of the Tethyan torn slabs were proposed to explain the surface strain and kinematics across both the Aegean–Anatolian and eastern Himalayan regions (e.g., Tapponnier and Molnar, 1976; Tapponnier et al., 1986; Jolivet et al., 1990; Royden, 1997; Armijo et al., 1999; Fournier et al., 2004; Becker and Faccenna, 2011). In addition, slab rollback is often proposed as a passive source of space to accommodate extrusion (e.g., Tapponnier et al., 1982; Armijo et al., 1999). However, the southward migration of the Hellenic trench is sensibly faster than the westward motion of Anatolia (Reilinger et al., 2010) (Fig. 1a), and classical extrusion models fail in predicting widespread extension such as that across the Ordos, Sichuan, Yunan regions in absence of a “free boundary” (e.g., Jolivet et al., 1990, 1994; Royden, 1997; Wang et al., 2001). These flaws suggest that slab rollback is in fact an active player and not just a passive source of space.

These geological, geophysical and geodetic observations, which provide insights on the long-term and recent geologic history, can constrain self-consistent three-dimensional (3D) numerical thermo-mechanical geodynamic models in order to achieve a first-order quantification of the relative contribution of the deep and shallow dynamics in setting the surface deformation across convergent plate boundaries. Previous numerical studies demonstrated along trench variations and complex mantle and crustal processes and surface deformation in subduction–collision systems (e.g., van Hunen and Allen, 2011; Capitanio and Replumaz, 2013;

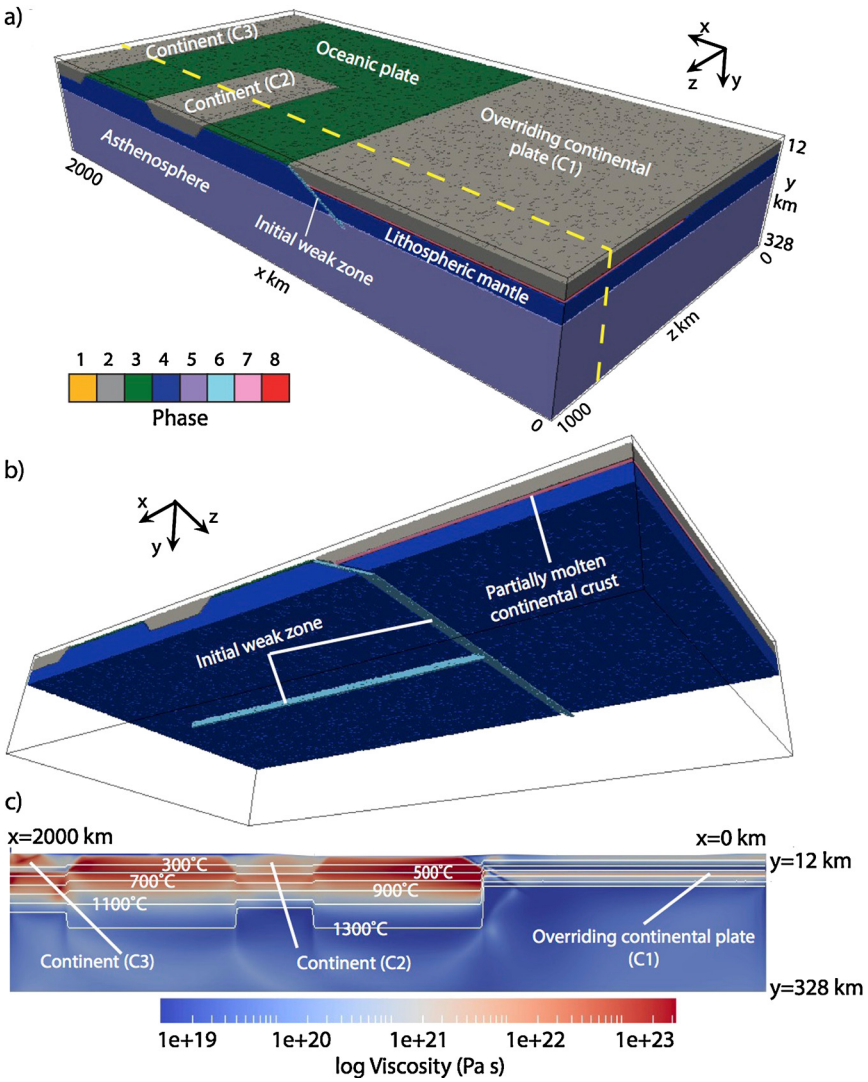

Fig. 2. Model setup. a) The 3D model domain (2000 × 328 × 1000 km in the x, y and z directions, respectively) with colours showing different rock types: 1 – sediments; 2 – continental crust; 3 – oceanic crust; 4 – lithospheric mantle; 5 – asthenospheric mantle; 6 – hydrated/serpentinized mantle (initially imposed "weak fracture zone"); 7 – partially molten continental crust; 8 – partially molten mantle. The top layer ("sticky air", $y < \sim 12$ km) and other phases are cut off for clarity. Convergence is imposed by applying uniform and constant-in-time velocity equal to ~ 1.8 cm yr^{-1} on the $x = 2000$ km model boundary. b) Initial model domain and location of the "weak zones" (i.e., hydrated/serpentinized mantle) into the lithosphere to initialise subduction (z-parallel) and allow slab tearing (x-parallel). The bottom layer (asthenosphere, $y > \sim 105$ km) is cut off for clarity. c) x–y viscosity profile of the initial model domain. The profile location is shown by the yellow dashed line in (a).

Li et al., 2013; Duretz et al., 2014). Although some implications for the large-scale tectonics across the Tethyan domain have been suggested (Li et al., 2013; Duretz et al., 2014), the relative contributions of crustal and mantle flow processes to surface deformation remained widely unaddressed.

2. Methods

The purpose of this paper is to assess the relative contributions of the lithospheric and mantle dynamics in setting the surface deformation at the transition between collisional and subduction domains. To this aim, we use 3D Cartesian thermo-mechanical modelling to resolve self-consistently the joint effects of oceanic subduction, slab tearing and continental collision on mantle flow and surface deformation at high resolution and accounting for realistic crustal and mantle rheologies. In addition to the reference model setup and boundary conditions, we outline below some of the principal features of the numerical model, but more detailed information can be found in Gerya and Yuen (2007), Zhu et al. (2009), Gerya (2010) and Li et al. (2013). Details on the parametric study can be found in the Supplementary Material.

2.1. 3D numerical model, setup and boundary conditions

All numerical experiments were performed with the code "I3ELVIS" (Gerya, 2010), solving the momentum, continuity and energy equations based on a staggered finite difference scheme combined with a marker-in-cell technique. Realistic and non-Newtonian visco-plastic rheologies (Ranalli, 1995) are used in the model. The model domain (Fig. 2) measures 2000 × 328 × 1000 km in the x, y and z dimensions, respectively. This domain is resolved by 501 × 165 × 197 grid points resulting in a resolution of 4, 2 and 5 km in the x, y and z dimensions, respectively. ~130 million randomly distributed markers are used for advecting the material properties and temperatures. The velocity boundary conditions are free slip at the top ($y = 0$ km) and at both the front and back boundaries ($z = 0$ km and $z = 1000$ km). The left and right boundaries ($x = 0$ km and $x = 2000$ km) use constant x-parallel velocities, which define the material influx. Global mass conservation is

Table 1
Material properties used in the numerical experiments. Qz. and Ol. correspond to the abbreviations of Quartzite and Olivine. k denotes the thermal conductivity, ρ_0 is the density, C_p is the specific heat capacity, E_a is the activation energy, V_a is the activation volume, n is the stress exponent, η_0 is the reference viscosity, Hr is the radiogenic heat production, ϕ_{eff} is the effective internal friction angle. Cohesion is 1 MPa for each phase.

Material	k ($W\,m^{-1}\,K^{-1}$)	ρ_0 ($kg\,m^{-3}$)	C_p ($J\,kg^{-1}\,K^{-1}$)	E_a ($kJ\,mol^{-1}$)	V_a ($m^3\,mol^{-1}$)	n	η_0 ($Pa^n\,s$)	Hr ($mW\,m^{-3}$)	Viscous flow law	$\sin(\phi_{eff})$
Sticky-air	20	1	100	0	0	1	1×10^{19}	0	Air	0
Water	20	1000	3330	0	0	1	1×10^{19}	0	Water	0
Sediment	$0.64 + 807/(T + 77)$	2600	1000	154	8	2.3	1.97×10^{17}	2	Wet Qz.	0.15
Cont. crust (C1, C3)	$0.64 + 807/(T + 77)$	2750	1000	154	8	2.3	1.17×10^{17}	2	Wet Qz.	0.15
Cont. crust (C2)	$1.18 + 807/(T + 77)$	2950	1000	238	8	3.2	4.8×10^{22}	2	Wet Qz.	0.15
Oc. crust	$1.18 + 474/(T + 77)$	3000	1000	238	8	3.2	4.8×10^{22}	0.25	Wet Qz.	0.15
Mantle	$0.73 + 1293/(T + 77)$	3300	1000	532	8	3.5	3.98×10^{16}	0.02	Dry Ol.	0.6
Weak zone	$0.73 + 1293/(T + 77)$	3300	1000	47	8	4	5×10^{20}	0.05	Wet Ol.	0

ensured by material outflux through the lower permeable boundary ($y = 328$ km). The top surface of the lithosphere is calculated dynamically as an internal free surface through a 12 km thick layer of "sticky air" (Gerya, 2010). Surface processes are implemented using a highly simplified gross-scale erosion–sedimentation law according to which instantaneous erosion limits mountains height to 4 km above the reference water level ($y = 12$ km), whereas instantaneous sedimentation limits trench depth to 8 km below the water level (Gerya and Yuen, 2007). The initial temperature gradient in the asthenospheric mantle is $\sim 0.5\,°C\,km^{-1}$ (adiabatic). The thermal boundary conditions are 0 °C for the upper boundary and nil horizontal heat flux across the vertical boundaries. An infinity-like external temperature condition (Gerya, 2010) is imposed on the lower boundary. All the numerical experiments were performed using 20 cores on the BRUTUS cluster at the ETH-Zürich (the approximate run time of a simulation is two weeks).

2.2. A joint model of continental collision, oceanic subduction and slab tearing

Our numerical experiments were not designed to reproduce any particular case, but can be applied to the transition between a continental indenter flanked by active oceanic subduction. We stress that the ultimate goal of our numerical experiments is to investigate the *effects* of slab tearing on the mantle and surface strain, but the potential *causes* of a tear in the slab are beyond the scope of this work. As such, we impose mechanical weaknesses in the oceanic plate and spatial variations of the upper continental crust (as detailed below), but do not claim that, in natural contexts, slab tears are necessarily generated by these factors.

The reference model is set up as follows. Three continental plates (C1, C2 and C3) are included into the initial model domain (Fig. 2a and Table 1). The crust of C2 and C3 are 50 km and 45 km thick, respectively. By varying the crustal thickness of the upper plate (C1) along the trench-parallel direction (z) one can control the slab descent rates (Nikolaeva et al., 2010) and therefore generate a tear in the slab. In particular, we imposed the crust of C1 as 35 km thick where $z \leq 490$ km and 45 km thick where $z > 510$ km (linear interpolation in between). The initial thermal structure of C1, C2 and C3 is laterally uniform with 0 °C at the surface and 1300 °C at 90, 140 and 150 km depth respectively. An oceanic domain, characterised by a trench-parallel weak fracture zone to initiate subduction and a trench-perpendicular weak fracture zone to allow for slab tearing, separates the three continental plates (Fig. 2a, b). The thermal structure of the oceanic lithosphere is that of a half-space cooling age of 120 Ma (e.g., Turcotte and Schubert, 2002). Uniform and constant in time x-parallel velocities equal to $\sim 1.8\,cm\,yr^{-1}$ (convergence) are imposed to the $x = 2000$ km boundary.

The evolution of the reference model is shown in Fig. 3 and in Video S1, S2 and S3. The details and timing of the model evolution depends upon the assumed thermal and mechanical parameters (see the Supplementary Materials), but the overall sequence of events (Fig. 3) is robust and includes: 1) early subduction of the oceanic domain between C1 and C2 and 2) later subduction of the oceanic domain between C1 and C3. These major events are allowed by tearing of the slab and separated in time by the collision between C1 and C2. Trench retreat, back-arc extension and progressive approach/collision of the continental plates characterise the surface evolution during the entire model run.

3. Results

In this section, we outline the numerical results with particular focus on the relationships between mantle and crustal flow and the effects of slab tearing and continental collision on the surface strain.

3.1. Mantle vs. crustal flow

A toroidal motion (with a minor ascending poloidal component) induced by the down-going slab dominates the deep dynamics during the first subduction event (Fig. 4a). This toroidal flow occurs both below C1 and through the opening slab window. At the surface, extensional and compressional deformation occurs in the back-arc and collisional domain, respectively. Crustal and mantle flows are essentially decoupled and surface deformation seems to be substantially driven by incipient slab rollback and trench retreat within the oceanic domain between C1 and C3 and continental collision between C1 and C2. The rheological stratification of the continental plates is essentially unaffected by this early subduction event, implying that the traction due to mantle flow is imposed at the base of the lithosphere (Fig. 4c).

The model evolution during the second subduction event is highly conditioned by the precedent toroidal flow of hot asthenosphere. This flow warmed the incipiently subducting lithosphere close to the slab tear, enhancing here slab rollback and trench retreat, generating a non-cylindrical (i.e., not parallel to the initial upper plate margin) subduction (Figs. 3, 4b and 4e). This subduction geometry induces a lateral (i.e., with non-nil trench-parallel component of motion), horizontal to sub-horizontal return flow of hot asthenospheric material, which further enhances the asymmetry of subduction (Fig. 4b). The surface deformation across C1 is characterised at this stage by a faster trench retreat in the proximity of the collisional domain and above the slab tear, while localised strike-slip deformation propagating toward the subducting plate as the model progresses accommodates the rotation of a crustal block (Figs. 3b and 4b). The rheological stratification of the upper plate in the back-arc extensional domain is characterised by the absence of a rigid lithospheric mantle and the velocity–depth profile shows particularly fast mantle flow (Fig. 4d), parallel in places to the surface velocity field (Fig. 4b). This translates into shear stresses (σ_{xy}) up to ~100 MPa applied directly to the base of the crust by the asthenospheric flow (Fig. 5).

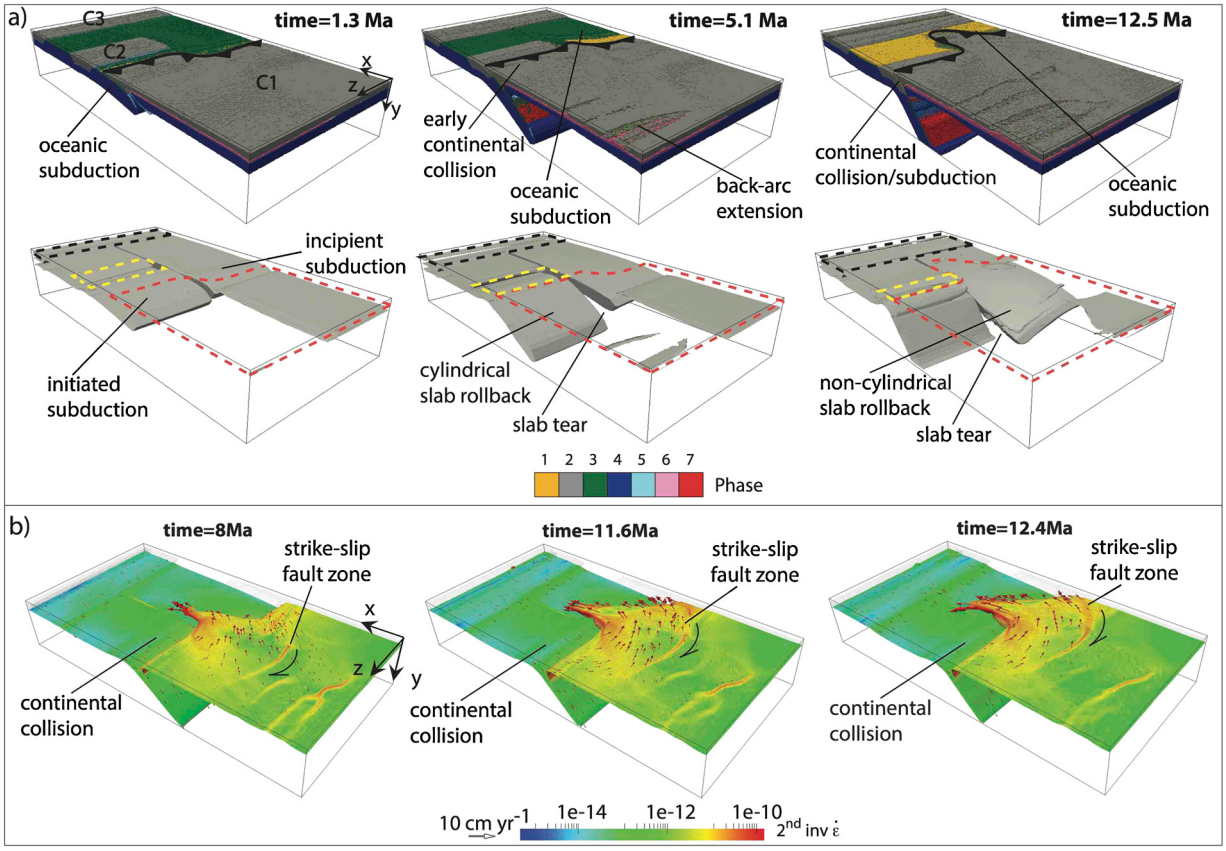

Fig. 3. Evolution of the reference model. a) Colours on the top panels show different rock types: 1 – sediments; 2 – continental crust; 3 – oceanic crust; 4 – lithospheric mantle; 5 – hydrated/serpentinized mantle (initially imposed "weak fracture zone"); 6 – partially molten continental crust; 7 – partially molten mantle. The top layer ("sticky-air", $y <\sim 12$ km), the asthenosphere and other phases are cut off for clarity. The subducting plates shown on the bottom panels are visualised through an iso-viscosity contour equal to 10^{22} Pa s. Red, yellow and black dashed lines on the lower panels show the plan view of C1, C2 and C3, respectively. b) Selected frames showing the 800 °C isotherm (mostly corresponding to the crust–lithospheric mantle transition within the C1 domain), colour-coded by the second invariant of the rate-of-strain tensor on this surface. A strike-slip fault zone (also visible at the surface, Fig. 4b) is generated by the sub-horizontal mantle flow (red arrows) following slab rollback and tearing. Note that the timing of panels in (a) and (b) is different.

3.2. *Effects of slab tearing and continental collision on the surface strain*

By comparing the reference model outputs to similar simulations, but not implying collision between C1 and C2 or slab tearing, one can decouple the first-order crustal and mantle contributions to the surface strain. It appears that strain localisation along a major strike-slip fault zone and thus the onset of a distinctive block-like deformation and surface rotation only occurs when both collision between rigid continental plates and slab tearing take place (Figs. 4b and 6). In particular, the trench parallel component of motion within the upper plate is sensibly reduced in absence of continental collision or slab tearing. Besides, slab tearing allows/enhances rollback of the subducting plate, trench parallel/toroidal migration of the asthenosphere, trench retreat and extension within the upper plate.

It is noteworthy that, when both continental collision and slab tearing allow for a block-like deformation and surface rotation, the velocity fields within the crust and mantle are sensibly faster within the back-arc extensional region and close to the subduction trench than in the collisional domain (Fig. 4b).

4. Discussion

Various combinations of processes such as extrusion tectonics, suction exerted by slab rollback, gravitational collapse of the collisional belt and mantle drag associated with regional plum-like upwelling were proposed to explain the observed surface kinematics across the Tethyan convergent domain (e.g., Tapponnier and Molnar, 1976; Royden, 1997; Armijo et al., 1999; Allen et al., 2004; Alvarez, 2010; Becker and Faccenna, 2011). Most of the proposed models, however, neglected the role played by the dynamical asthenospheric flow originated by slab rollback and tearing. A major outcome of our numerical experiments is that the toroidal motion of the asthenosphere at the edge of a retreating tearing slab is able to modulate the thermal state of the lithosphere, in turn affecting the geometry and dynamics of later subduction events and associated mantle and surface strain. Tectonic inheritance is clearly not a new concept, but it most often refers to the mechanical properties of the lithosphere and mantle (e.g., Thomas, 2006), while we show here that also the thermal and kinematic inheritances can significantly affect the surface evolution. Moreover, the mantle return flow following slab rollback and tearing is able to produce tectonically significant (i.e., up to ∼100 MPa; Bürgmann and Dresen, 2008) shear stresses at the base of the lithosphere and crust. Thus, surface strain across subduction zones is likely to be jointly driven by slab rollback and mantle flow, especially across hot and thinned environments, characterised by the absence of a rigid mantle lithosphere such as the back-arc domains. It was demonstrated that the horizontal traction generated at the base of deep continental roots from regional thermal anomalies within the mantle dragged the continents together along the Tethyan axis and was able to protract convergence even after continental collision and brake-off of the

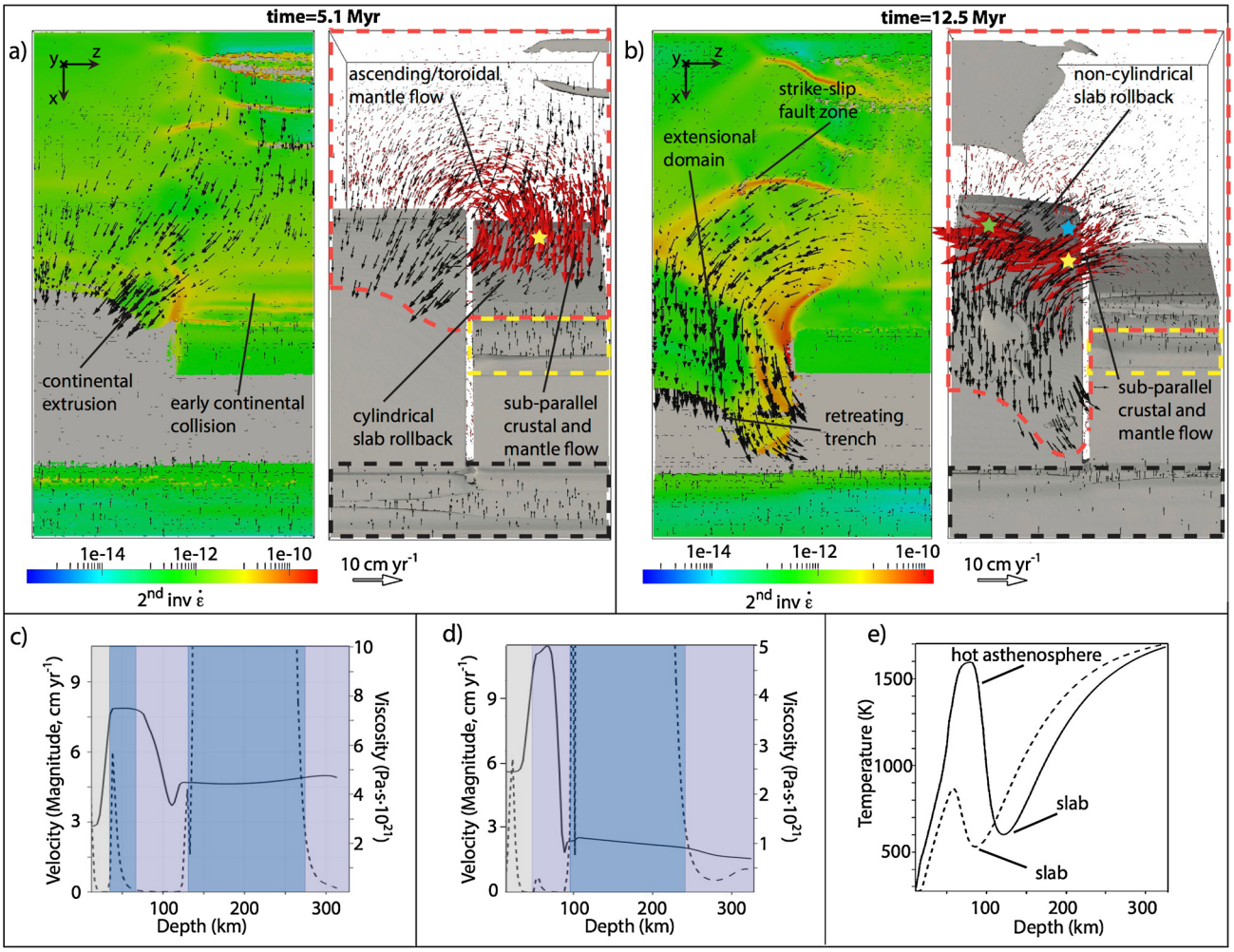

Fig. 4. a–b) Plan view of selected temporal frames. Black and red arrows represent the velocity vectors in the continental crust and asthenosphere, respectively. Colours on the left panel show the second invariant of the rate-of-strain tensor. The subducting plates are shown on the right panel through an iso-viscosity contour equal to 10^{22} Pa s. Red, yellow and black dashed lines on the right panels show the plan view of C1, C2 and C3, respectively. c–d) Depth–velocity–viscosity profiles (y-parallel). The profile location is shown by the yellow stars in (a) and (b). Solid lines, representing the magnitude of the velocity vector, follow the left-axis. Dashed lines, representing the viscosity, follow the right-axis. Shaded background colours show the phase at each depth: grey – continental crust, blue – lithospheric mantle/slab, and purple – asthenospheric mantle. e) Temperature–depth profiles at 12.5 Ma (the green and blue stars in (b) show the locations of the dashed and solid profile, respectively).

Tethyan slabs (Alvarez, 2010). The sub-horizontal mantle flow then seems to be able to actively drive the surface strain and kinematics across both thin and thick continental lithospheres. As such, the sub-horizontal couplings between the Earth's mantle and surface should benefit from the same attention that is paid to the vertical couplings and associated "dynamic topography" (e.g., Braun, 2010).

Our numerical experiments show that the surface strain at the transition between a continental indenter and an oceanic subduction can be dominated by the suction exerted by slab rollback (enhanced by slab tearing) and the associated mantle flow, as demonstrated by faster crustal flow close to the subduction trench than to the collisional domain (Fig. 4b). Although the continental indenter is necessary for setting a block-like deformation and surface rotation, its role is that of a passive bulwark if the overall convergence rates are slower than slab rollback. Thus, the effectiveness of extrusion tectonics, crustal shortening and gravitational collapse at the margins of a collisional belt should be assessed in the light of the dynamics of the neighbouring oceanic subduction (Fig. 7), since the "free boundary" is the most important factor controlling these mechanisms.

We cannot resolve the timing of slab tearing across the Aegean–Anatolian or the eastern Indian–Eurasian margins nor can we address its relationships to slab rollback or continental collision through our modelling. However, trench migration rates are inversely correlated to the width of the subducting plate (Schellart et al., 2007), which implies that the observed tears decoupling the actively subducting slabs from the mantle lithosphere below the collisional domains might have facilitated slab rollback and modulated trench retreat after continental collision, consistently with our numerical experiments. A common feature in the Mediterranean metamorphic core complexes exhumed in back-arc domains from the lower and middle crust is a highly asymmetric deformation with constant sense of shear – i.e., hangingwall motion relative to footwall (Jolivet et al., 2008, 2009). Our modelling results suggest that this asymmetric deformation is substantially controlled by the basal shear stresses imposed to the crust by the asthenospheric return flow.

The modelled surface velocity field shown in Fig. 4b is also similar (regardless of the sense of spin) to the observed surface rotation across the Aegean–Anatolian and the eastern Indian–Eurasian margins (Fig. 1). The majority of the observed surface rotation across the natural examples is accommodated by several fault zones amongst which the NAF, the Kun-Lun, Xianshuihe-Xiaojiang and the Altyn Tagh faults (e.g., Sengör, 1979; Tapponnier et al., 1982), whose kinematics is reasonably well reproduced in our numerical experiments by highly localised strike-slip deformation

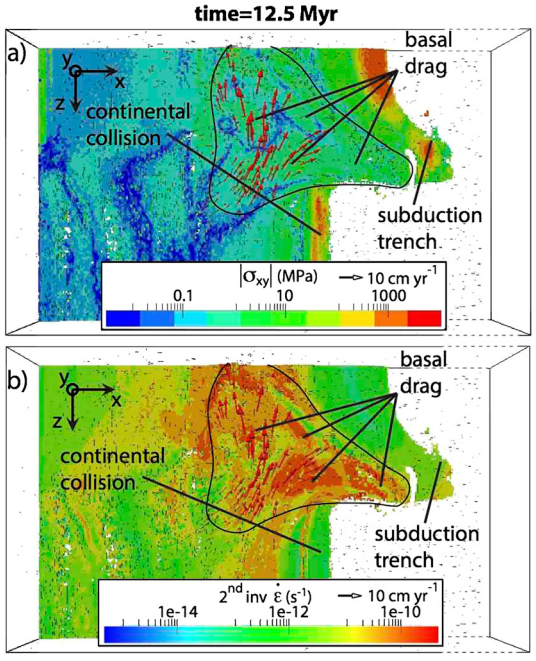

Fig. 5. Shear stress (a) and strain rate (b) distribution at the base of the upper plate continental crust (C1) at 12.5 Myr modelled time on the reference simulation. Red arrows show the velocity field within the asthenosphere. The area inside the black line is where the asthenosphere is at direct contact with the base of the continental crust.

(Figs. 3 and 4b). A faster crustal flow close to the subduction trench than to the collisional domain in our reference model is consistent with GPS measurements across the Aegean–Anatolian region, and suggests that the Aegean extension and extrusion of Anatolia are principally driven by the subduction dynamics and associated mantle flow, instead of collision-related mechanisms (Fig. 7). The arrival of the Australian plate to the Sumatra trench in middle-late Miocene times (Ricou, 1994) might have reduced the suction exerted by oceanic subduction. Nonetheless, the crust along portions of southeastern Tibet has been extending since at least ~4 Myr (e.g., Royden, 1997; Wang et al., 2001). The many basins and low topographies across the Sichuan, Yunan, Indochina and Sunda provinces as well as the back-arc basins further testify widespread extension, implying that the Andaman–Sumatra and other western Pacific subduction zones substantially affected the surface strain across southeastern Asia during most of the Cenozoic (Jolivet et al., 1990). In addition, tomographic models highlight the presence of hot and shallow asthenospheric material across southeastern Tibet (e.g., Li et al., 2008a, 2008b), which is analogous to the asthenosphere flowing at direct contact with the base of the crust and rotating around the edge of the collisional domain in our numerical experiments. Since a free boundary seems necessary to allow for continental extrusion (e.g., Tapponnier and Molnar, 1976; Tapponnier et al., 1982; Jolivet et al., 1990; Fournier et al., 2004) and this free boundary is provided by oceanic subduction which we proved able to actively drive the surface strain more efficiently than the continental indentation, our experiment confirm that the rollback of the Andaman–Sumatra and the associated mantle return flow actively determined the surface strain east and southeast of the EHS (Fig. 7).

Instantaneous global flow models calculated from mantle density anomalies, suggest that both the pull from the Tethyan slabs and mantle upwelling from underneath the Ethiopia–Afar and Reunion–Carlsberg regions are necessary to reproduce the crustal motion across the Tethyan collisional belts (Becker and Faccenna, 2011; Faccenna et al., 2013a, 2013b; Faccenna and Becker, 2010). Our results suggest that the dynamical mantle flow associated solely with slab rollback and tearing can produce a distinct block-like surface rotation, without the intervention of an external dragging force such as the upwelling from the lower mantle. In our models, however, slab tearing is triggered along the pre-existing weak oceanic fracture zones and modelled slabs are not tied to previously subducted plates as the Tethyan slabs probably were during most of the Cenozoic (Ricou, 1994). Mantle upwellings, thus, have a major role in setting crustal motion at the scale of the whole Tethyan margins by dragging the northern and southern

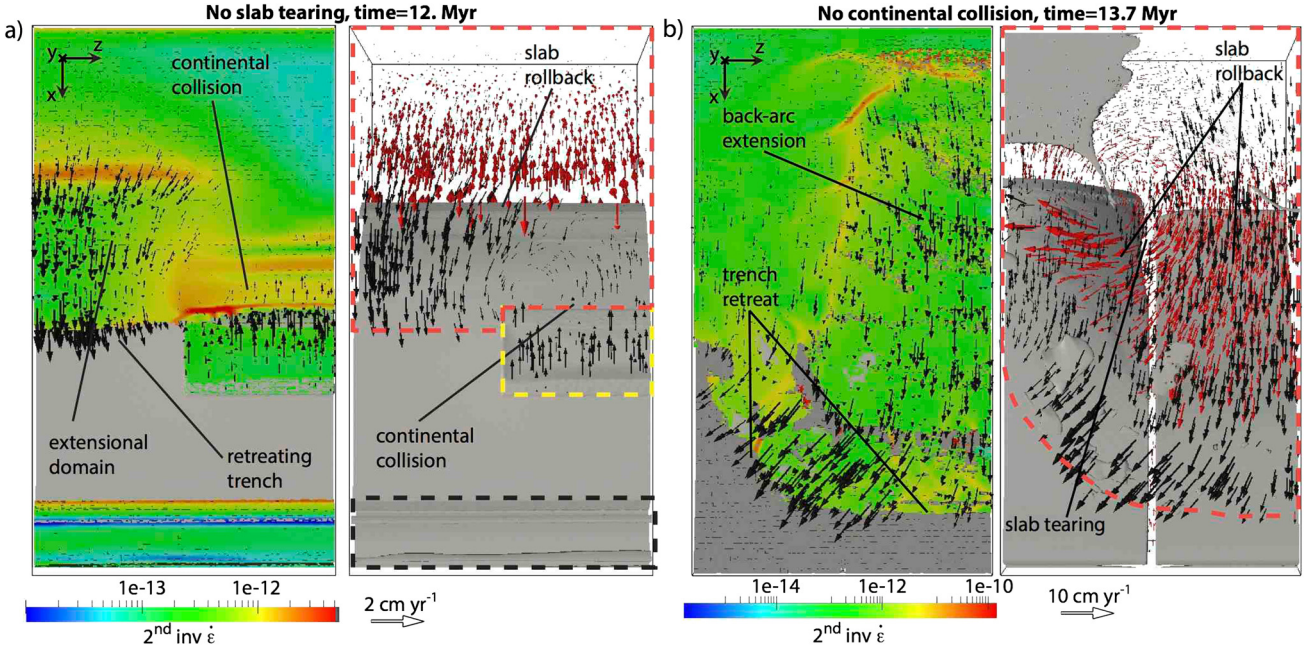

Fig. 6. a) Plan view of a selected temporal frame of a simulation without slab tearing. b) Plan view of a selected temporal frame of a simulation without continental collision. Black and red arrows represent the velocity vectors in the continental crust and asthenosphere, respectively. Colours on the left panels show the second invariant of the rate-of-strain tensor. The subducting plates are shown on the right panel through an iso-viscosity contour equal to 10^{22} Pa s. Red, yellow and black dashed lines on the right panels show the plan view of C1, C2 and C3, respectively.

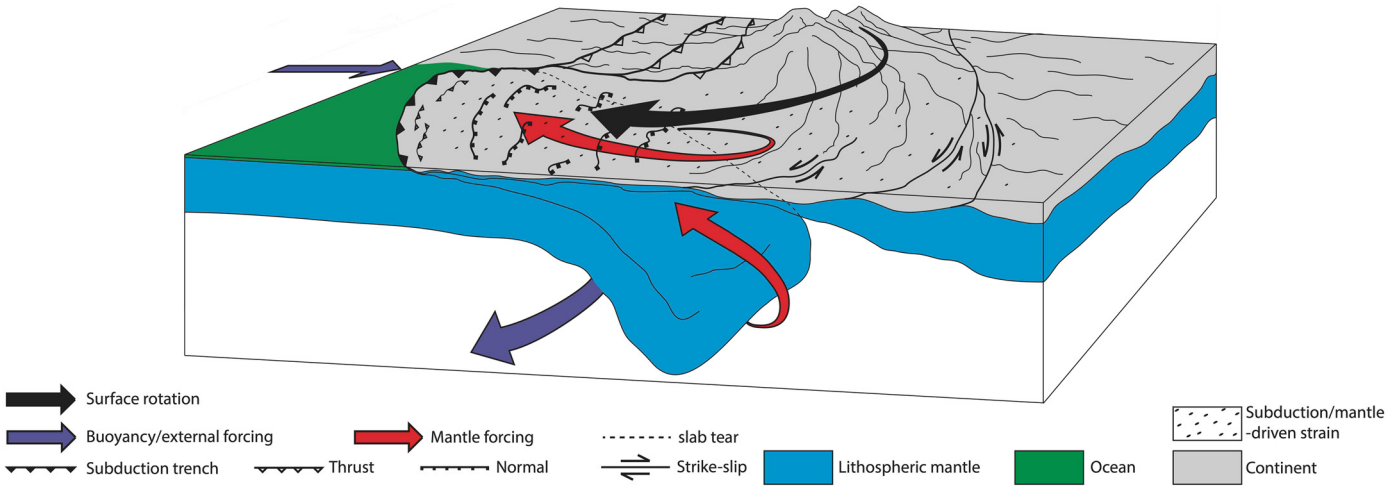

Fig. 7. Illustrative representation of the dynamical interactions between continental collision, oceanic subduction, mantle flow and surface deformation.

continents together along the Tethyan axis (Alvarez, 2010), warming and propelling the upper continental plates (Becker and Faccenna, 2011; Faccenna et al., 2013a, 2013b; Faccenna and Becker, 2010) and, possibly, by thermally enhancing slab tearing, but the rollback of the Tethyan slabs and the associated mantle return flow are likely to be the primary drivers of the surface deformation at the edge of the Tethyan collisional belts.

5. Conclusions

3D Cartesian thermo-mechanical models of self-consistent oceanic subduction, slab tearing and continental collision calibrated on geologic, geophysical and geodetic observations and accounting for realistic crustal and mantle rheologies enabled us to conclude that:

- The dynamical asthenospheric flow originated by slab rollback and tearing is a primary factor controlling the surface evolution at the transition between collisional and subduction domains. In particular, the toroidal motion of the asthenosphere at the edge of a retreating tearing slab is able to modulate the thermal state of the lithosphere, in turn affecting the geometry and dynamics of later subduction events and associated mantle and surface strain. In addition, the sub-horizontal mantle return flow following slab rollback and tearing is able to produce tectonically significant shear stresses at the base of the lithosphere and crust. The surface strain across subduction zones is thus likely to be jointly driven by slab rollback and mantle flow, especially across hot and thinned environments such as the back-arc domains.
- The surface strain at the transition between a continental indenter and an oceanic subduction can be dominated by the suction exerted by slab rollback (enhanced by slab tearing) and the associated mantle flow. The continental indenter acts as a passive bulwark if the overall convergence rates are slower than slab rollback. Thus, the effectiveness of extrusion tectonics, crustal shortening and gravitational collapse at the margins of a collisional belt should be assessed in the light of the dynamics of the neighbouring oceanic subduction.
- A faster crustal flow close to the Hellenic subduction trench than to the collisional domain (consistently reproduced by our numerical models) suggests that the suction exerted by the Hellenic subduction and associated mantle flow is the principal driver of the Aegean extension and extrusion of Anatolia, instead of currently proposed collision-related mechanisms. Our experiment also confirm that the rollback of the Andaman–Sumatra and the associated mantle return flow affected the surface strain east and southeast of the EHS as also suggested by the several basins and low topographies across the Sichuan, Yunan, Indochina and Sunda provinces, which testify widespread extension.
- Mantle upwelling drag and propel the northern and southern continents along the Tethyan axis and possibly thermally enhance slab tearing. The rollback of the Tethyan slabs and the associated mantle return flow, however, are likely to be primary drivers of the surface deformation at the edge of the Tethyan collisional belts.

Acknowledgements

This work has been financially supported by the Laboratoire d'Excellence (LABEX) VOLTAIRE (Convention n° ANR-10-LABX-100-01) of the University of Orléans and the European Research Council (ERC) under the 7th Framework Programme of the European Union (ERC Advanced Grant, grant agreement No. 290864, RHEOLITH). Numerical simulations were performed on the ETH-Zürich cluster BRUTUS. We are thankful to Claudio Faccenna and Thorsten Becker for stimulating discussions and to Kosuke Ueda for constructive comments on an early version of the manuscript and tips for the modelling. The paper benefited from insightful revision by Leigh Royden and two anonymous reviewers.

Appendix A. Supplementary material

Supplementary material related to this article can be found online at http://dx.doi.org/10.1016/j.epsl.2014.08.023.

References

Allen, M., Jackson, J., Walker, R., 2004. Late Cenozoic reorganization of the Arabia–Eurasia collision and the comparison of short-term and long-term deformation rates. Tectonics 23. http://dx.doi.org/10.1029/2003TC001530.

Alvarez, W., 2010. Protracted continental collisions argue for continental plates driven by basal traction. Earth Planet. Sci. Lett. 296, 434–442.

Armijo, R., Meyer, B., Hubert, A., Barka, A., 1999. Westward propagation of the north Anatolian into the northern Aegean: timing and kinematics. Geology 27 (3), 267–270.

ArRajehi, A., McClusky, S., Reilinger, R., Daoud, M., Alchalbi, A., Ergintav, S., Gomez, F., Sholan, J., Bou-Rabee, F., Ogubazghi, G., Haileab, B., Fisseha, S., Asfaw, L., Mahmoud, S., Rayan, A., Bendik, R., Kogan, L., 2010. Geodetic constraints on present

day motion of the Arabian Plate: implications for Red Sea and Gulf of Aden rifting. Tectonics 29, TC3011. http://dx.doi.org/10.1029/2009TC002482.
Becker, T., Faccenna, C., 2011. Mantle conveyor beneath the Tethyan collisional belt. Earth Planet. Sci. Lett. 310, 453–461.
Braun, J., 2010. The many surface expressions of mantle dynamics. Nat. Geosci. 3, 825–833.
Bürgmann, R., Dresen, G., 2008. Rheology of the lower crust and upper mantle: evidence from rock mechanics, geodesy, and field observations. Annu. Rev. Earth Planet. Sci. 36, 531–567.
Capitanio, F., Replumaz, A., 2013. Subduction and slab breakoff controls on Asian indentation tectonics and Himalayan western syntaxis formation. Geochem. Geophys. Geosyst. 14 (9), 3515–3531.
De Boorder, H., Spakman, W., White, S.H., Wortel, M.J., 1998. Late Cenozoic mineralization, orogenic collapse and slab detachment in the European Alpine Belt. Earth Planet. Sci. Lett. 164 (3), 569–575.
Dewey, J.F., 1988. Lithospheric stress, deformation, and tectonic cycles: the disruption of Pangaea and the closure of Tethys. Geol. Soc. (Lond.) Spec. Publ. 37 (1), 23–40.
Duretz, T., Gerya, T., Spakman, W., 2014. Slab detachment in laterally varying subduction zones: 3D numerical modeling. Geophys. Res. Lett. http://dx.doi.org/10.1002/2014GL059472.
Faccenna, C., Becker, T., 2010. Shaping mobile belts by small-scale convection. Nature 465, 602–605.
Faccenna, C., Becker, T.W., Conrad, C.P., Husson, L., 2013a. Mountain building and mantle dynamics. Tectonics 32, 80–93.
Faccenna, C., Becker, T., Jolivet, L., Keskin, M., 2013b. Mantle convection in the Middle East: reconciling Afar upwelling, Arabia indentation and Aegean trench rollback. Earth Planet. Sci. Lett. 375, 254–269.
Faccenna, C., Bellier, O., Martinod, J., Piromallo, C., Regard, V., 2006. Slab detachment beneath eastern Anatolia: a possible cause for the formation of the North Anatolian fault. Earth Planet. Sci. Lett. 242, 85–97.
Fournier, M., Jolivet, L., Davy, P., Thomas, J., 2004. Backarc extension and collision: an experimental approach to the tectonics of Asia. Geophys. J. Int. 157 (2), 871–889.
Gan, W., Zhang, P., Shen, Z., Niu, Z., Wang, M., Wan, Y., Zhou, D., Cheng, J., 2007. Present day crustal motion within the Tibetan Plateau inferred from GPS measurements. J. Geophys. Res. 113.
Gerya, T., 2010. Introduction to Numerical Geodynamic Modelling. Cambridge University Press.
Gerya, T., Yuen, D., 2007. Robust characteristics method for modelling multiphase visco-elasto-plastic thermo-mechanical problems. Phys. Earth Planet. Inter. 163, 83–105.
Govers, R., Wortel, M.J., 2005. Lithosphere tearing at STEP faults: response to edges of subduction zones. Earth Planet. Sci. Lett. 236, 505–523.
Holt, W.E., 2000. Correlated crust and mantle strain fields in Tibet. Geology 28 (1), 67–70.
Jolivet, L., Augier, R., Faccenna, C., Negro, F., Rimmele, G., Agard, P., Robin, C., Rossetti, F., Crespo-Blanc, A., 2008. Subduction, convergence and the mode of backarc extension in the Mediterranean region. Bull. Soc. Géol. Fr. 179 (6), 525–550.
Jolivet, L., Davy, P., Cobbold, P., 1990. Right-lateral shear along the Northwest Pacific Margin and the India–Eurasia Collision. Tectonics 9 (6), 1409–1419.
Jolivet, L., Faccenna, C., 2000. Mediterranean extension and the Africa–Eurasia collision. Tectonics 19.
Jolivet, L., Faccenna, C., Piromallo, C., 2009. From mantle to crust: stretching the Mediterranean. Earth Planet. Sci. Lett. 285, 198–209.
Jolivet, L., Tamaki, K., Fournier, M., 1994. Japan Sea, opening history and mechanism, a synthesis. J. Geophys. Res. 99, 22237–22259.
Jolivet, L., Faccenna, C., Huet, B., Labrousse, L., Le Pourhiet, L., Lacombe, O., Lecompte, E., Burov, E., Denèle, Y., Brun, J.-P., et al., 2013. Aegean tectonics: strain localization, slab tearing and trench retreat. Tectonophysics 597–598, 1–33.
Le Pichon, X., Fournier, M., Jolivet, L., 1992. Kinematics, topography, shortening and extrusion in the India–Eurasia collision. Tectonics 11 (6), 1085–1098.
Li, C., van der Hilst, R., Engdahl, E.R., Burdick, S., 2008a. A new global model for P wave speed variations in Earth's mantle. Geochem. Geophys. Geosyst. 9 (5).
Li, C., van der Hilst, R., Meltzer, A.S., Engdahl, E.R., 2008b. Subduction of the Indian lithosphere beneath the Tibetan Plateau and Burma. Earth Planet. Sci. Lett. 274, 157–168.
Li, Z., Xu, Z., Gerya, T., Burg, J.P., 2013. Collision of continental corner from 3-D numerical modeling. Earth Planet. Sci. Lett. 380, 98–111.
McKenzie, D.P., 1972. Active tectonics of the Mediterranean region. Geophys. J. R. Astron. Soc. 30, 109–185.
Molnar, P., Tapponnier, P., 1975. Cenozoic tectonics of Asia: effects of a continental collision. Science 189 (4201), 419–426.
Nikolaeva, K., Gerya, T., Marques, F.O., 2010. Subduction initiation at passive margins: numerical modeling. J. Geophys. Res. 115. http://dx.doi.org/10.1029/2009JB006549.
Pérouse, E., Chamont-Rooke, N., Rabaute, A., Briole, P., Jouanne, F., Georgiev, I., Dimitrov, D., 2012. Bridging onshore and offshore present-day kinematics of central and eastern Mediterranean: implications for crustal dynamics and mantle flow. Geochem. Geophys. Geosyst. 13 (9). http://dx.doi.org/10.1029/2012GC004289.
Ranalli, G., 1995. Rheology of the Earth, Deformation and Flow Processes in Geophysics and Geodynamics. Chapman & Hall.
Reilinger, R., McClusky, S., Paradissis, D., Ergintav, S., Vernant, P., 2010. Geodetic constraints on the tectonic evolution of the Aegean region and strain accumulation along the Hellenic subduction zone. Tectonophysics 488, 22–30.
Replumaz, A., Guillot, S., Villaseñor, A., Negredo, M., 2013. Amount of Asian lithospheric mantle subducted during the India/Asia collision. Gondwana Res. 24, 936–945.
Ricou, L.E., 1994. Tethys reconstructed: plates, continental fragments and their boundaries since 260 Ma from Central America to South-Eastern Asia. Geodin. Acta 7 (4), 169–218.
Royden, L.H., 1993. The tectonic expression slab pull at continental convergent boundaries. Tectonics 12 (2), 303–325.
Royden, L., 1997. Surface deformation and lower crustal flow in Eastern Tibet. Science 276.
Royden, L.H., Burchfiel, B.C., van der Hilst, R.D., 2008. The geological evolution of the Tibetan Plateau. Science 321, 1054–1058.
Schellart, W.P., Freeman, J., Stegman, D.R., Moresi, L., May, D., 2007. Evolution and diversity of subduction zones controlled by slab width. Nature 446, 308–311.
Sengör, A.M., 1979. The North Anatolian transform fault: its age, offset and tectonic significance. J. Geol. Soc. (Lond.) 136, 269–282.
Tapponnier, P., Molnar, P., 1976. Slip-line field theory and large scale continental tectonics. Nature 264, 319–324.
Tapponnier, P., Peltzer, G., Le Dain, A.Y., Armijo, R., Cobbold, P., 1982. Propagating extrusion tectonics in Asia: new insights from simple experiments with plasticine. Geology 10, 611–616.
Tapponnier, P., Peltzer, G., Armijo, R., 1986. On the mechanics of the collision between India and Asia. In: Coward, M.P., Ries, A.C. (Eds.), Collision Tectonics, pp. 115–157.
Tapponnier, P., Zhiqin, X., Roger, B., Meyer, B., Arnaud, N., Wittlinger, G., Jingsui, Y., 2001. Oblique stepwise rise and growth of the Tibet plateau. Science 294 (5547), 1671–1677.
Taylor, B., Hayes, D.E., 1983. Origin and history of the South China Sea basin. In: Hayes, D.E. (Ed.), The Tectonic and Geologic Evolution of Southeast Asian Seas and Islands, Part 2. AGU, Washington, D.C., pp. 23–56.
Thomas, W.A., 2006. Tectonic inheritance at a continental margin. GSA Today 16 (2).
Turcotte, D.L., Schubert, G., 2002. Geodynamics. Cambridge University Press, Cambridge.
van Hunen, J., Allen, M.B., 2011. Continental collision and slab break-off: a comparison of 3-D numerical models with observations. Earth Planet. Sci. Lett. 203 (1–2), 27–37.
Wang, Q., Zhang, P., Freymueller, J.T., Bilham, R., Larson, K.M., Lai, X., You, X., Niu, Z., Wu, J., Li, Y., Liu, J., Yang, Z., Chen, Q., 2001. Present-day crustal deformation in China constrained by global positioning system measurements. Science 194.
Zhang, Z.K., Wang, M., Gan, W., Bürgmann, R., Wang, Q., Niu, Z., Sun, J., Wu, J., Hanrong, S., Xinzhao, Y., 2004. Continuous deformation of the Tibetan Plateau from global positioning system data. Geology 32, 809–812.
Zhu, G., Gerya, T.V., Yuen, D.A., Honda, S., Yoshida, T., Connolly, J.A., 2009. 3-D dynamics of hydrous thermal–chemical plumes in oceanic subduction zones. Geochem. Geophys. Geosyst. 10, Q11006.